Modelling Soil Erosion and Bed Formation in Shallow Overland Flow

Christiana Mavroyiakoumou

University of Oxford

A case study report submitted for the degree of

M.Sc. in Mathematical Modelling and Scientific Computing

Hilary 2017

1 Introduction

The aim of this report is to describe water overland flow in terms of a mathematical model to see how this flow influences the soil. In particular, we want to investigate soil erosion on the bed (surface) of the land.

Firstly, soil erosion refers to the phenomenon that causes soil degradation as a consequence of wind or water effects. We will consider the latter in this report. More specifically, water flowing down a slope causes soil erosion and as water waves propagate they tend to form rills. Within these rills, instabilities tend to grow in the soil, creating periodic wave-like structures that travel upstream (antidunes) if $Fr > 1$, or downstream (dunes) if $Fr < 1$, as shown in Figure 1.1. For more details on what the Froude number (Fr) is, see Appendix B. Note that in this project we have assumed that the flux of water, q ($\mathrm{m}^2\ \mathrm{s}^{-1}$), flowing down a slope is constant and that the water layer is shallow. The main objective is to model the formation of antidunes in shallow overland flow.

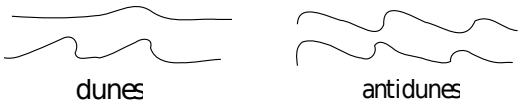

Figure 1.1: Subcritical and supercritical flow. See Appendix B.

Many mathematical models have been developed in an attempt to make predictions of erosion rates as a function of the various interactions that cause soil erosion in the first place. Here we consider the Hairsine-Rose (HR) erosion model [2]. The HR model is unique in that it deals with the effect of particle size distribution and distinguishes between deposited non-cohesive soil and original cohesive soil. In particular, the model assumes that there exist I particle size classes. Considering particles of different sizes establishes a more realistic model that enables better predictions to be made on how overland flow affects soil particles of different sizes, rather than assuming that the soil consists of a single uniform particle size.

This report is organised as follows: In Section 2, we introduce the HR model. Then in Section 3, we simplify the model by non-dimensionalising it, finding the travelling wave solution and reducing the coupled PDE system to the leading order ODE system. The leading order system is further reduced by integrating the equations that have decoupled. Finally, in Section 4, the existence of hydraulic jumps is demonstrated by carrying out numerical simulations. In particular, we reproduce [3, Figure 7.29] and study the effect of changing parameters such as bed slope and overland flow rate. Some of the details are relegated to the appendices.

2 The HR Model

Hairsine and Rose [2] developed a soil erosion model that includes the processes of rainfall, detachment, entrainment and sediment deposition. Figure 2.1 shows the flow diagram for these different processes as they are visualised by the HR model.

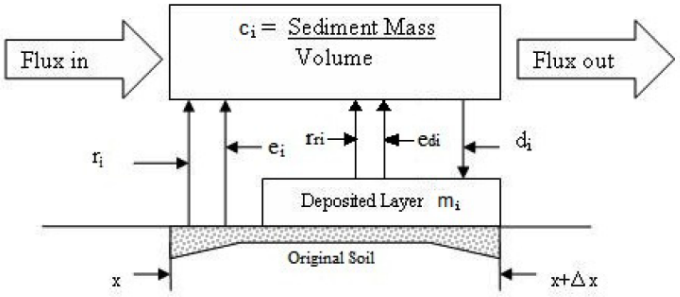

Figure 2.1: Flow diagram describing the interaction of soil erosion processes between the sediment flux, the original soil and the deposited layer, taken from [2].

Furthermore, Figure 2.2 shows a sketch of the flow geometry used in the model. Most importantly, the height of the water is denoted by h (m), the water flux by $q = uh$ (m^2 s^{-1}) and the velocity of the water by u (m s^{-1}). Moreover, in Figure 2.2, z_D represents the reference height, z_m represents the deposited layer height and finally, z_b represents the height of the cohesive soil layer.

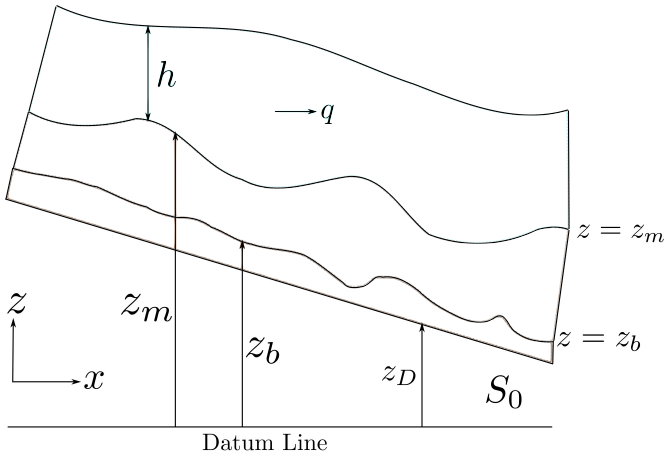

Figure 2.2: A sketch of the model and flow geometry.

In the following subsections, we will describe the individual components and equations that constitute the HR model as they appear in [3].

2.1 Entrainment and Detachment

Entrainment describes the removal of sediment from the original uneroded soil by the action of overland flow. The rate of entrainment of sediment from the original soil is r_i (kg m^{-2} s^{-1}) for each size class i and is given by

$$r_i = \frac{F}{J} p_i (1 - H)(\Omega - \Omega_{\text{cr}}), \tag{2.1}$$

where p_i is the proportion of sediment of size class i of the original uneroded soil and $p \in (0, 1]$. Its components are described below. Entrainment depends on the stream power[1] of the flow. For a plane with slope S_0, the stream power per unit width of flow, Ω, is given by

$$\Omega = \rho g S_0 q \tag{2.2}$$

and has units (W m^{-2}). Here ρ is the density of the water (kg m^{-3}), g is acceleration due to gravity (m s^{-2}) and q is the water flux (m^2 s^{-1}).

In Figure 2.3, we show how the potential energy of the excess rainfall is distributed.

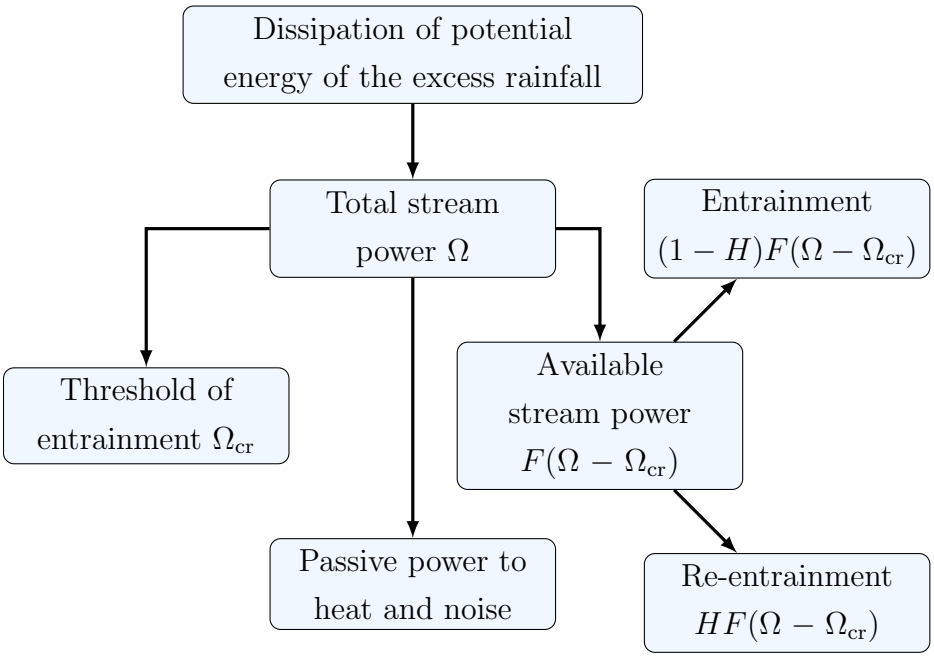

Figure 2.3: Flow diagram of the use of the potential energy.

Note that there is a critical stream power Ω_{cr} below which no soil is entrained or re-entrained and that some of the excess stream power $(\Omega - \Omega_{\text{cr}})$ is lost through

[1]Stream power is the rate of work of the mutual shear stress between the soil surface and the overland flow and represents the power per unit area available to get work done.

heat or noise. Moreover, F represents the fraction of $(\Omega - \Omega_{\text{cr}})$ which is available for entrainment and re-entrainment. Now, we define the *protection factor*, H, which is provided by the deposited layer as

$$H = \min\left(1, \frac{m}{m^\star}\right) = \begin{cases} \frac{m}{m^\star}, & m < m^\star, \\ 1, & m > m^\star, \end{cases} \tag{2.3}$$

where $m^\star$ is a threshold mass that determines the value of H. So $H \in [0, 1]$, with $H = 0$ corresponding to no deposited layer and $H = 1$ corresponding to fully covered original soil. Note that in this report we assume that $H = 1$.

Since the soil particles in the original soil are bound together by cohesive forces, we define a parameter J (J kg^{-1}) as the specific energy of entrainment[2]. The rate of entrainment is driven by the effective excess stream power $(1 - H)F(\Omega - \Omega_{\text{cr}})$, and the rate of re-entrainment is driven by the rest of the effective excess stream power, which is $HF(\Omega - \Omega_{\text{cr}})$.

The rate of detachment e_i (kg m^2 s^{-1}) is given by

$$e_i = a(h)p_i P(1 - H), \tag{2.4}$$

where P is the rainfall rate, and $a(h)$ is the flow depth-dependent soil detachability coefficient and it is a property of the soil.

2.2 Soil Equations

Now we write equations that describe the bed formation and evolution. We initially consider multiple particle sizes and concentrations c_i, $i = 1, ..., I$, where I is the number of particle size classes.

2.2.1 Mass Conservation for Suspended Sediment and Deposited Layer

The one-dimensional HR model equation for suspended sediment concentration c_i is given by

$$\frac{\partial}{\partial t}(hc_i) + \frac{\partial}{\partial x}(qc_i) = r_i + r_{ri} - d_i. \tag{2.5}$$

Soil is 'added' to sediment by overland flow lifting it off from the cohesive layer at a rate r_i, or by lifting it off the deposited layer at a rate r_{ri}. Soil is 'lost' when it falls to the bed at a rate d_i. Note that all of these rates are dependent on the particle size.

[2] J is the energy per unit mass required to break the soil particle into individual size classes.

Let m_i denote the mass that particle type i contributes to the deposited layer. The mass conservation equation can thus be written as

$$\frac{\partial m_i}{\partial t} = d_i - r_{ri}. \tag{2.6}$$

Note that here, deposited sediment is 'lost' from water at a rate r_{ri} and 'added' to it at a rate d_i.

2.3 Re-Entrainment, Re-Detachment and Deposition

Overland flow acting on the deposited layer which is now covering the soil surface causes re-entrainment. Bonds in the cohesive soil have been broken down and are thus negligible, and the original soil has turned into deposited soil. So the force resisting the removal of soil by the flow is dependent on the suspended sediment weight. This is proportional to $\frac{\rho_s - \rho}{\rho_s}$, where ρ_s (kg m^{-3}) is the density of the sediment and ρ (kg m^{-3}) is the density of the water. The re-entrainment rate, r_{ri} (kg m^{-2} s^{-1}), is

$$r_{ri} = \frac{F}{gh}\frac{\rho_s}{\rho_s - \rho} H(\Omega - \Omega_{\text{cr}})\frac{m_i}{m}, \tag{2.7}$$

and the rate of re-detachment, e_{di} (kg m^2 s^{-1}), is given by

$$e_{di} = a_d(h) P H \frac{m_i}{m}, \tag{2.8}$$

where $a_d(h)$ is the flow soil detachability coefficient for the deposited layer.

Deposition relates to the action of gravity on the suspended sediment. The suspended sediment falls on the soil surface due to its weight and it increases the height of the deposited layer. The deposition rate, d_i (kg m^{-2} s^{-1}), is therefore given by

$$d_i = v_i c_i, \tag{2.9}$$

where v_i is the fall velocity for each size class and c_i is the suspended sediment concentration.

2.4 Water Equations – St. Venant Equations

The St. Venant equations are a pair of mass and momentum equations given by

$$\frac{\partial h}{\partial t} + \frac{\partial q}{\partial x} = 0, \tag{2.10}$$

$$\frac{\partial q}{\partial t} + \frac{\partial}{\partial x}\left(\frac{q^2}{h} + \frac{gh^2}{2}\right) = gh(S_0 - S_f), \tag{2.11}$$

where $S_0 = -\frac{\partial z_D}{\partial x}$ is the bed slope and $S_f = \frac{c_r u^2}{h^k}$ is the friction factor[3].

[3]Note that k and c_r are different depending on what friction law is being used, i.e. Chézy is $k = 1$ and $c_r = \frac{f}{g}$ or Manning is $k = \frac{4}{3}$ and $c_r = n^2$.

2.5 Soil Interface Equations

At this point we need to introduce the equations that describe the evolution of soil interfaces between the cohesive and the deposited soil layer and also between the deposited soil and the water layer. The two equations are given by

$$\rho_s(1-\phi_m)\,\frac{\partial(z_m - z_b)}{\partial t} = \sum_{i=1}^{I}(d_i - r_{ri}), \tag{2.12}$$

$$\rho_s(1-\phi_b)\,\frac{\partial(z_b - z_D)}{\partial t} = -\sum_{i=1}^{I} r_i, \tag{2.13}$$

and are often referred to as the Exner equations. Here the constant ϕ_b defines the porosity of the cohesive soil and ϕ_m the porosity of the deposited layer. The height above the datum reference slope is given by $z = \frac{m_t}{(1-\phi)\rho_s}$, where m_t is the total mass of suspended sediment particles.

Below we summarise our HR model equations.

Summary of HR Model Equations

Water mass conservation:
$$\frac{\partial h}{\partial t} + \frac{\partial q}{\partial x} = 0 \tag{2.14}$$

Water momentum conservation:
$$\frac{\partial q}{\partial t} + \frac{\partial}{\partial x}\left(\frac{q^2}{h} + \frac{gh^2}{2}\right) = gh(S_0 - S_f) \tag{2.15}$$

Deposited soil layer:
$$\rho_s(1-\phi_m)\frac{\partial(z_m - z_b)}{\partial t} = \sum_{i=1}^{I} v_i c_i - \frac{F}{g}\frac{H}{h}\frac{\rho_s}{\rho_s - \rho}(\Omega - \Omega_{\text{cr}})\frac{m_i}{m_t} \tag{2.16}$$

Cohesive soil layer:
$$\rho_s(1-\phi_b)\frac{\partial(z_b - z_D)}{\partial t} = -\sum_{i=1}^{I}\frac{F}{J}p_i(1-H)(\Omega - \Omega_{\text{cr}}) \tag{2.17}$$

Suspended sediment:
$$\frac{\partial(hc_i)}{\partial t} + \frac{\partial(qc_i)}{\partial x} = \frac{F}{J}p_i(1-H)(\Omega - \Omega_{\text{cr}}) + \frac{F}{g}\frac{H}{h}\frac{\rho_s}{\rho_s - \rho}(\Omega - \Omega_{\text{cr}})\frac{m_i}{m_t} - v_i c_i \tag{2.18}$$

Bed sediment:
$$\frac{\partial m_i}{\partial t} = v_i c_i - \frac{F}{g}\frac{H}{h}\frac{\rho_s}{\rho_s - \rho}(\Omega - \Omega_{\text{cr}})\frac{m_i}{m_t} \tag{2.19}$$

A summary of the constants that appear in the HR model can be found in Appendix C.

3 Simplifying the Model

In this section, we treat the model to include multiple particle size classes but our code is programmed to deal with a single particle size class. For a single particle size class, note that quantities like $\frac{m_i}{m}$ become 1 and all the quantities with an index i lose this index.

3.1 Non-Dimensionalisation

We carry out appropriate non-dimensionalisation on the full HR model (2.14)–(2.19) to simplify it in order to be able to work with it more easily. In particular, we non-dimensionalise the model using the following scales (by choosing $z_0 = h_0$) and parameters:

$$m_0 = h_0\rho_s(1-\phi_m) = v_0c_0t_0,\ c_0 = \frac{F\Omega_0}{gh_0v_0}\frac{\rho_s}{\rho_s-\rho},\ z_0 = h_0 = \frac{F\Omega_0}{gv_0c_0}\frac{\rho_s}{\rho_s-\rho},\ \Omega_0 = \frac{\rho g h_0 q_0 \delta}{x_0},$$
$$A = \frac{h_0 g(\rho_s-\rho)}{J\rho_s},\ \delta = \frac{c_r u_0^3}{v_0 h_0^k},\ Fr^2 = \frac{q^2}{gh^3},\ \varepsilon = \frac{h_0}{v_0t_0} = \frac{c_0}{\rho_s(1-\phi_m)}, \beta = \frac{1-\phi_b}{1-\phi_m}.$$

Here, Fr is a measure of how rapid the flow is and β is the ratio of porosities of the soil layers. Suitable non-dimensionalisation leads to the dimensionless Exner equations for the interface of the deposited layer and the original soil, respectively,

$$\frac{\partial(z_m - z_b)}{\partial t} = \sum_{i=1}^{I}\left[v_ic_i - \frac{H}{h}(\Omega-\Omega_{\text{cr}})\frac{m_i}{m_t}\right], \tag{3.1}$$

$$\beta\frac{\partial(z_b - z_D)}{\partial t} = -\sum_{i=1}^{I} Ap_i(1-H)(\Omega-\Omega_{\text{cr}}). \tag{3.2}$$

The dimensionless forms of the mass conservation equations in water are

$$\varepsilon\frac{\partial(hc_i)}{\partial t} + \frac{\partial(qc_i)}{\partial x} = Ap_i(1-H)(\Omega-\Omega_{\text{cr}}) + \frac{H}{h}(\Omega-\Omega_{\text{cr}})\frac{m_i}{m_t} - v_ic_i, \tag{3.3}$$

$$\frac{\partial m_i}{\partial t} = v_ic_i - \frac{H}{h}(\Omega-\Omega_{\text{cr}})\frac{m_i}{m_t}. \tag{3.4}$$

Finally, the St. Venant equations for mass and momentum conservation to describe overland flow reduce to

$$\varepsilon\frac{\partial h}{\partial t} + \frac{\partial q}{\partial x} = 0, \tag{3.5}$$

$$\varepsilon Fr^2\frac{\partial q}{\partial t} + \frac{\partial}{\partial x}\left(Fr^2\frac{q^2}{h} + \frac{h^2}{2}\right) = h\left(-\frac{\partial z_m}{\partial x} + \delta\frac{u^2}{h^k}\right), \tag{3.6}$$

where h is the flow depth, q is the unit discharge and z_m is the bed elevation.

Note that since we wish to investigate the development of instabilities and bed formation, the time scale should be chosen with regards to the bed evolution equation for the deposited soil layer (2.16). The scale is determined by setting the coefficient of the time derivative to be equal to 1 and is given by

$$t_0 = \frac{z_0 \rho_s (1 - \phi_m)}{v_0 c_0}. \tag{3.7}$$

We choose the length scale by balancing the advection and deposition rates in (2.18). Note that v_0 is the average fall velocity and is given by $v_0 = \frac{1}{I}\sum_{i=1}^{I} v_i$. The scale is found as $x_0 = \frac{q_0}{v_0}$. Similarly, we choose the mass scale, m_0, from (2.19).

3.2 Travelling Wave Solution

The motivation behind introducing a shock is that we want to approximate the rapid, periodic increase in the height of the water layer above the bed form that occurs in flumes or experiments. Subsequently we move to the frame of reference of the shock moving with speed s and we define the travelling wave coordinate as

$$\xi = x + \lambda t, \tag{3.8}$$

where λ represents the wave speed[4]. This way we simplify the system of PDEs to a system of ODEs. In Figure 3.1, L is the wavelength ($L = \xi_+ - \xi_-$) and h_-, h_+ are the heights before and after the hydraulic jump, respectively. The arrow below λ in Figure 3.1 shows the direction in which the shock propagates.

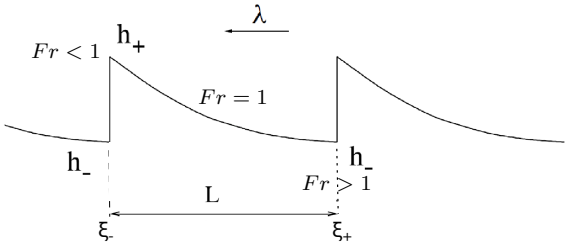

Figure 3.1: Schematic diagram of hydraulic jump modified from [3].

3.3 Hydraulic Jump Conditions (Rankine-Hugoniot)

Shocks are described by interpreting the equations in a weak form and returning to the conservation arguments from which the equations were derived. This way we can

[4]If we perform a change of variables then we obtain $\frac{\partial}{\partial t} = \frac{\mathrm{d}}{\mathrm{d}\xi}\frac{\partial \xi}{\partial t} = \lambda \frac{\mathrm{d}}{\mathrm{d}\xi}$ and $\frac{\partial}{\partial x} = \frac{\mathrm{d}}{\mathrm{d}\xi}\frac{\partial \xi}{\partial x} = \frac{\mathrm{d}}{\mathrm{d}\xi}$.

describe the shock speeds, s, using the Rankine-Hugoniot conditions, which yields

$$s = \frac{[q]_-^+}{[\varepsilon h]_-^+}, \; s = \frac{[Fr^2u^2h + \frac{1}{2}h^2]_-^+}{[\varepsilon Fr^2 q]_-^+}, \; s = \frac{[qc_i]_-^+}{[\varepsilon h c_i]_-^+}. \tag{3.9}$$

The first and third conditions in (3.9) imply that we require $c_i^+ = c_i^-$, or, equivalently that concentration is continuous through the hydraulic jump.

3.4 Reduction to Leading Order System

Note that we can write a leading order system by letting the parameters $A \to 0$, $\Omega_{\text{cr}} \to 0$ and $\varepsilon \to 0$. These are verified from experimental data[5]. Note that we assume that Ω_{cr} has to be very low for soil to have the ability to be entrained.

If we do this then the system of equations from Subsection 3.1 for Manning's law $\left(k = \frac{10}{3}\right)$ simplifies to

Water mass conservation:
$$q = uh = 1, \tag{3.10}$$

Water momentum conservation:
$$\frac{\mathrm{d}}{\mathrm{d}\xi}\left(\frac{Fr^2}{h} + \frac{h^2}{2}\right) = -h\left(\frac{\mathrm{d}\hat{z}_m}{\mathrm{d}\xi} - \delta + \frac{\delta}{h^{\frac{10}{3}}}\right), \tag{3.11}$$

Suspended sediment:
$$\frac{\mathrm{d}c_i}{\mathrm{d}\xi} = \frac{H}{h}\Omega\frac{m_i}{m_t} - v_i c_i, \tag{3.12}$$

Bed sediment:
$$\lambda\frac{\mathrm{d}m_i}{\mathrm{d}\xi} = -\frac{\mathrm{d}c_i}{\mathrm{d}\xi}, \tag{3.13}$$

Deposited soil layer:
$$\lambda\frac{\mathrm{d}\hat{z}_m}{\mathrm{d}\xi} = \lambda\sum_{i=1}^{I}\frac{\mathrm{d}m_i}{\mathrm{d}\xi} = \lambda\frac{\mathrm{d}m_t}{\mathrm{d}\xi}. \tag{3.14}$$

Note that we have used $z_m = \hat{z}_m + \delta(L - x) = \hat{z}_m + z_D$, and that $m_t = \sum_{i=1}^{I} m_i$.

It is evident that we can integrate (3.13) to obtain

$$\lambda m_i + c_i = \psi_i, \tag{3.15}$$

where ψ_i is the constant of integration and we can also integrate (3.14) to get

$$\lambda\hat{z}_m = \lambda m = \psi - c. \tag{3.16}$$

So it is easy to solve equations (3.10), (3.13) and (3.14), but equations (3.11) and (3.12) are coupled for h and c, so they require more work.

If we rearrange the water momentum equation (3.11) as

$$-\frac{Fr^2}{h^2}\frac{\mathrm{d}h}{\mathrm{d}\xi} + h\frac{\mathrm{d}h}{\mathrm{d}\xi} = h\left(\delta + \frac{1}{\lambda}\frac{\mathrm{d}c}{\mathrm{d}\xi} - \frac{\delta}{h^{10/3}}\right), \tag{3.17}$$

[5]In [3] typical values for these parameters appear to be: $A = 0.12$ and $\varepsilon = 0.043$.

where we used that $\frac{\mathrm{d}\hat{z}_m}{\mathrm{d}\xi} = -\frac{1}{\lambda}\frac{\mathrm{d}c}{\mathrm{d}\xi}$, we can write

$$\frac{\mathrm{d}h}{\mathrm{d}\xi}\left(-\frac{Fr^2}{h^2}+h\right) = \frac{\mathrm{d}h}{\mathrm{d}\xi}\left(\frac{-Fr^2+h^3}{h^2}\right) = h\left(\delta + \frac{1}{\lambda}\frac{\mathrm{d}c}{\mathrm{d}\xi} - \frac{\delta}{h^{10/3}}\right). \tag{3.18}$$

This coupled system for both the concentration and the height of the hydraulic jump is given by

$$\frac{\mathrm{d}h}{\mathrm{d}\xi} = \frac{h^3}{h^3 - Fr^2}\left(\delta + \frac{1}{\lambda}\frac{\mathrm{d}c}{\mathrm{d}\xi} - \frac{\delta}{h^{10/3}}\right). \tag{3.19}$$

However, (3.19) becomes singular when $h^3 = Fr^2$ which means that at this critical height, $h_c = Fr^{2/3}$, we need to set

$$\left(\delta + \frac{1}{\lambda}\frac{\mathrm{d}c}{\mathrm{d}\xi} - \frac{\delta}{h^{10/3}}\right)\Bigg|_{h=h_c} = 0, \tag{3.20}$$

since $h(\xi)$ is a smooth function apart from the hydraulic jump position.

We know that this singularity can be achieved in the first place since the flow goes from subcritical ($Fr < 1$) at h_+ to supercritical ($Fr > 1$) at h_- and so there is a point (in the middle possibly) where it achieves $Fr = 1$. This means that h can at some point obtain this critical value h_c. But we would like to remove the singularity that occurs at $h = h_c$, or equivalently the singularity that occurs at $\theta = 1$. Using (3.12) and after some manipulations that can be found in Appendix D, we write

$$\frac{\mathrm{d}c}{\mathrm{d}\xi} = \frac{H}{h^{13/3}} - \sum_{i=1}^{I} v_i c_i. \tag{3.21}$$

If we substitute this into (3.20) then we obtain

$$\lambda\delta + \frac{\Omega_c}{h_c} - \sum_{i=1}^{I} v_i c_i^c - \frac{\lambda\delta}{h_c^{10/3}} = 0 \tag{3.22}$$

and so (3.19) becomes

$$h_c^{16/3}\lambda\frac{\mathrm{d}\theta}{\mathrm{d}\xi} = \frac{\theta^3}{\theta^3-1}\left[h_c^{13/3}\sum_{i=1}^{I} v_i(c_i^c - c_i) + \frac{1}{\theta^{13/3}}\left(H - \theta^{13/3}\right) - \frac{\lambda\delta h_c}{\theta^{10/3}}\left(1-\theta^{10/3}\right)\right]. \tag{3.23}$$

For a detailed derivation of (3.23), see Appendix D. Let us note that for the rest of this section we will assume that the protection factor takes the value $H = 1$ and in the case of single class particle size we would have that v_i scales to 1.

We factorise $\theta^3 - 1 = (\theta^2+\theta+1)(\theta-1)$, so (3.23) can be written as

$$h_c^{16/3}\lambda\frac{\mathrm{d}\theta}{\mathrm{d}\xi} = \frac{h_c^{13/3}\theta^3}{\theta^2+\theta+1}\left[\frac{\sum_{i=1}^{I} v_i(c_i^c - c_i)}{\theta-1}\right] + \frac{1-\theta^{13/3}}{\theta^{4/3}(\theta^3-1)} - \lambda\delta h_c\frac{\left(1-\theta^{10/3}\right)}{\theta^{1/3}(\theta^3-1)}. \tag{3.24}$$

For that we assume that we can write the following series expansion

$$\frac{\sum_{i=1}^{I} v_i(c_i^c - c_i)}{\theta - 1} = a_0 + a_1(\theta - 1), \tag{3.25}$$

meaning that the whole equation can now be reduced to

$$h_c^{16/3}\lambda\frac{\mathrm{d}\theta}{\mathrm{d}\xi} = b_0 + b_1(\theta - 1). \tag{3.26}$$

The task now is to determine the constants a_0, a_1, b_0 and b_1.

The solution of (3.26) subject to $\theta = 1$, $\xi = \xi_c$ is found using an integrating factor of the form $\exp\left(-\frac{b_1}{h_c^{16/3}\lambda}\xi\right)$ and the series expansion of the exponential function. Details on the derivation of (3.27) can be found in Appendix F. Integrating the first order differential equation (3.26) yields

$$\theta - 1 = \frac{b_0}{\lambda h_c^{16/3}}(\xi - \xi_c) + \frac{b_0 b_1}{2\lambda^2 h_c^{32/3}}(\xi - \xi_c)^2. \tag{3.27}$$

Equivalently, if we solve [6] for $(\xi - \xi_c)$ instead, shows that the solution can also be given by

$$\xi - \xi_c = \frac{\lambda h_c^{16/3}}{b_0}(\theta - 1) - \frac{b_1\lambda h_c^{16/3}}{2b_0^2}(\theta - 1)^2. \tag{3.28}$$

Note that the above was done for the case of Manning's law. For Chézy's law, see [3]. Below we present the single size class solution for both types of friction laws. See Appendix A for more details on Manning's and Chézy's friction laws.

Manning	**Chézy**
$a_0 = -\frac{\lambda h_c^{16/3}}{b_0}\frac{\mathrm{d}c(\xi_c)}{\mathrm{d}\xi}$	$a_0 = -\frac{\lambda h_c^{5}}{b_0}\frac{\mathrm{d}c(\xi_c)}{\mathrm{d}\xi}$
$a_1 = \frac{b_1\lambda h_c^{16/3}}{2b_0^2}\frac{\mathrm{d}c(\xi_c)}{\mathrm{d}\xi} - \frac{\lambda^2 h_c^{32/3}}{2b_0^2}\frac{\mathrm{d}^2c(\xi_c)}{\mathrm{d}\xi^2}$	$a_1 = -\frac{b_1\lambda h_c^{5}}{2b_0^2}\frac{\mathrm{d}c(\xi_c)}{\mathrm{d}\xi} - \frac{\lambda^2 h_c^{10}}{2b_0^2}\frac{\mathrm{d}^2c(\xi_c)}{\mathrm{d}\xi^2}$
$c^c = \lambda\delta(1 - h_c^{-10/3}) + h_c^{-13/3}$	$c^c = \lambda\delta(1 - h_c^{-3}) + h_c^{-4}$
$\frac{\mathrm{d}c(\xi_c)}{\mathrm{d}\xi} = h_c^{-13/3} - c^c$	$\frac{\mathrm{d}c(\xi_c)}{\mathrm{d}\xi} = h_c^{-4} - c^c$
$\frac{\mathrm{d}^2c(\xi_c)}{\mathrm{d}\xi^2} = -\frac{13b_0}{3\lambda h_c^{29/3}} - \frac{\mathrm{d}c(\xi_c)}{\mathrm{d}\xi}$	$\frac{\mathrm{d}^2c(\xi_c)}{\mathrm{d}\xi^2} = -\frac{4b_0}{\lambda h_c^{9}} - \frac{\mathrm{d}c(\xi_c)}{\mathrm{d}\xi}$
$b_0 = \frac{h_c^{13/3}}{3}a_0 + \frac{10}{9}\lambda\delta h_c - \frac{13}{9}$	$b_0 = \frac{h_c^{4}}{3}a_0 + \lambda\delta h_c - \frac{4}{3}$
$b_1 = \frac{h_c^{13/3}}{3}(a_1 + 2a_0) - \frac{5}{27}\lambda\delta h_c + \frac{26}{27}$	$b_1 = \frac{h_c^{4}}{3}(a_1 + 2a_0) + \frac{2}{3}$

[6] Since it is a quadratic equation for $(\xi - \xi_c)$.

To determine what these constants should be, we first solve quadratically for b_0 and this fixes a_0. Once λ is chosen then c^c is determined and subsequently $\frac{\mathrm{d}c(\xi_c)}{\mathrm{d}\xi}$. Equations for a_0 and b_0 become two equations in two unknowns, i.e. a quadratic for either unknown. Now, $\frac{\mathrm{d}^2c}{\mathrm{d}\xi^2}(\xi_c)$ is also determined since we have λ, h_c, b_0 and $\frac{\mathrm{d}c}{\mathrm{d}\xi}(\xi_c)$. This in turn allows us to find b_1 and a_1. For more details, see Appendix E.

4 Numerical Procedure

In this section, we explain how to find a solution for the coupled system of equations

$$\frac{\mathrm{d}h}{\mathrm{d}\xi} = \frac{1}{\lambda}\frac{h^3}{h^3 - h_c^3}\left(\lambda\delta - \lambda\delta h^{-10/3} + h^{-13/3} - c\right), \tag{4.1}$$

$$\frac{\mathrm{d}c}{\mathrm{d}\xi} = h^{-13/3} - c, \tag{4.2}$$

if we are given the wave speed, λ. We start by presenting the constraints on the solution which arise from the Rankine-Hugoniot conditions of Subsection 3.3:

$$\left[\frac{Fr^2}{h} + \frac{h^2}{2}\right]\Bigg|_{\xi=0} = \left[\frac{Fr^2}{h} + \frac{h^2}{2}\right]\Bigg|_{\xi=L} \quad \text{and} \quad c(\xi = 0) = c(\xi = L). \tag{4.3}$$

For the solution to be unique, Zhong [3] concluded that a further condition needs to be satisfied, in the form of a mass conservation of the suspended sediment

$$\frac{1}{L}\int_0^L c(\xi)\,\mathrm{d}\xi = 1. \tag{4.4}$$

The numerical procedure must, therefore, ensure that the conditions (4.3a), (4.3b) and (4.4) are all satisfied and that the solution passes through the critical concentration $c^c = \lambda\delta(1 - h_c^{-10/3}) + h_c^{-13/3}$ and the critical height $h_c = Fr^{2/3}$. At the same time, we find a wavelength range $[\xi_-, \xi_+]$. We continually modify λ to satisfy all 3 conditions.

In the numerical scheme, we fix the wave speed λ and then we produce data, $h(\xi)$ and $c(\xi)$. For the analytic expansion we substitute $\theta = 1 + \varepsilon$ and $\theta = 1 - \varepsilon$ in (3.28) and then integrate numerically using the `MATLAB` function **ODE45**. Finally, we check that all 3 conditions are satisfied. The best values of ξ_- and ξ_+ are chosen for the given λ and the error for this is recorded.

4.1 Numerical Results

Firstly, in Figure 4.1, we reproduce [3, Figure 7.29] where the parameters used were:

$$h_0 = z_0 = 0.0895\,\mathrm{m},\ q_0 = 0.1097\,\mathrm{m}^2\,\mathrm{s}^{-1},\ n = 0.02,\ S_0 = 0.015,\ g = 9.81\,\mathrm{m}\,\mathrm{s}^{-2},$$

$$Fr = 1.3077,\ v_0 = 0.4,\ \delta = 0.046.$$

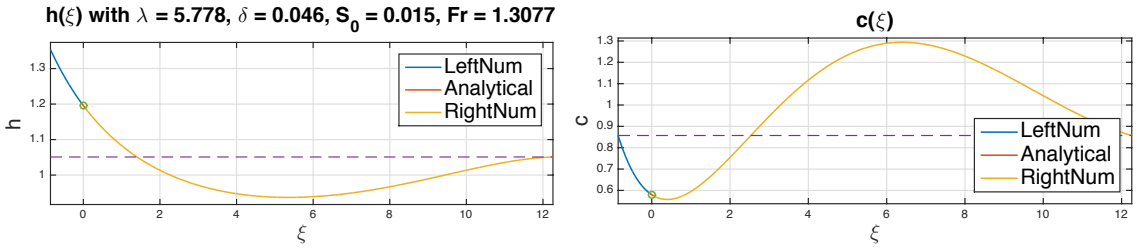

Figure 4.1: Best value: $\lambda = 5.778$, with L2-error $= 0.00048$ and $\xi \in [-0.86, 12.26]$.

It is worth noting that the solution here, as in [3], is provided based on Manning's friction law but can easily be changed to use Chézy's friction law instead.

The circle at $\xi = 0$ corresponds to the singularity at $h = h_c = Fr^{2/3}$. The blue part of the profile corresponds to the part of the wave upstream of the singularity where we integrate numerically. The very small red part in the circle is where we expand analytically around the singularity. Finally, the yellow part is where we integrate numerically for the part of the wave that is downstream of the singularity.

Furthermore, the dashed lines indicate where the conditions are satisfied. In the $h(\xi)$ vs. ξ plot, they correspond to the downstream height which satisfies (4.3a). In the $c(\xi)$ vs. ξ plot, the dashed lines indicate the downstream and upstream positions where the concentrations before and after the hydraulic jump are equal. This is condition (4.3b). Moreover, note that the scale on the horizontal axis corresponds to the wavelength which satisfies the mass conservation condition (4.4).

These plots are actually the solutions for a given pair of bed slope and flow rate.

4.2 Two-Parameter Family

In this subsection, we investigate the effect of varying parameters[7] that determine how overland flow affects bed formation. From the scalings found when we non-dimensionalised the model, we have

$$\delta = \frac{x_0 S_0}{h_0} = \frac{n^2 u_0^3}{v_0 h_0^{4/3}} \quad \text{and} \quad x_0 = \frac{q_0}{v_0} = \frac{u_0 h_0}{v_0}, \tag{4.5}$$

where δ is the bed slope and it is thus a factor of the bed geometry. Equivalently, it can be thought of as a measure of the roughness of the bed.

If we replace $u_0 = \frac{q_0}{h_0}$ in (4.5a) and rearrange to solve for h_0, then we obtain

$$h_0 = \frac{n^{3/5} q_0^{3/5}}{S_0^{3/10}}. \tag{4.6}$$

[7]Require $Fr > 1$ since this is the Froude range for which instabilities occur.

This gives the two-parameter family, where the two parameters are Fr^2 and δ. For Manning's friction law, these are given by

$$Fr^2 = \frac{u_0^2}{gh_0} = \frac{q_0^2}{gh_0^3} = \frac{S_0^{9/10} q_0^{1/5}}{gn^{9/5}} \quad \text{and} \quad \delta = \frac{n^2 q_0^3}{v_0 h_0^{13/3}} = \frac{S_0^{13/10} q_0^{2/5}}{v_0 n^{3/5}}. \tag{4.7}$$

Here note that $v_0 = 1$ for a single size class.

If we fix q_0 and n, then increasing S_0 increases Fr^2 as we can see from (4.7a). If now instead of increasing S_0, we increase q_0 by a suitable factor, then we get the same Fr^2 but different δ. This implies that we have here a two-parameter family of solutions instead of a one-parameter family.

In Figure 4.2, we study the effect of varying S_0 with q_0 fixed, or varying q_0 while S_0 is fixed making sure that Fr^2 matches.

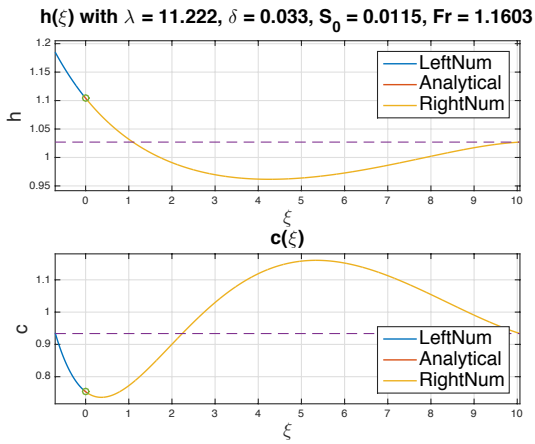

(a) Fix $q_0 = 0.1097$ and vary $S_0 = 0.0115$

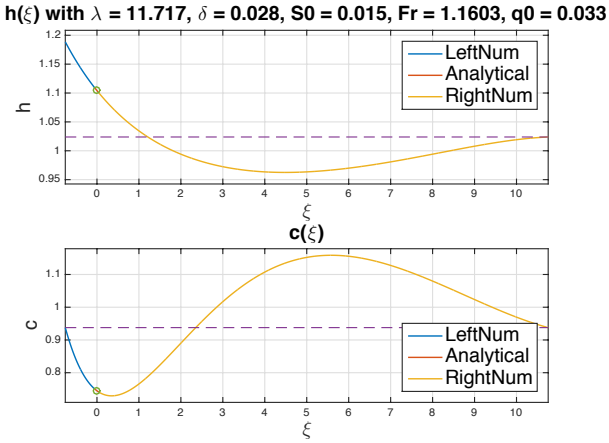

(b) Fix $S_0 = 0.0150$ and vary $q_0 = 0.033$

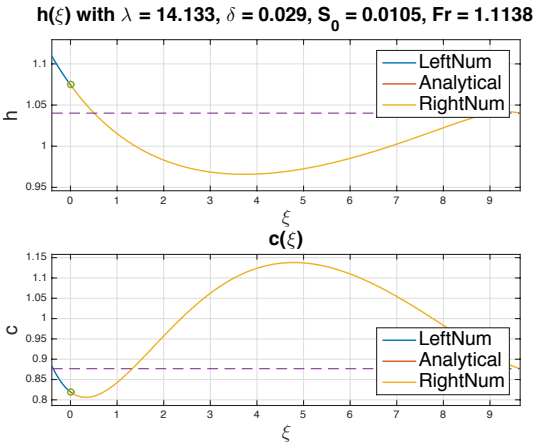

(c) Fix $q_0 = 0.1097$ and vary $S_0 = 0.0105$

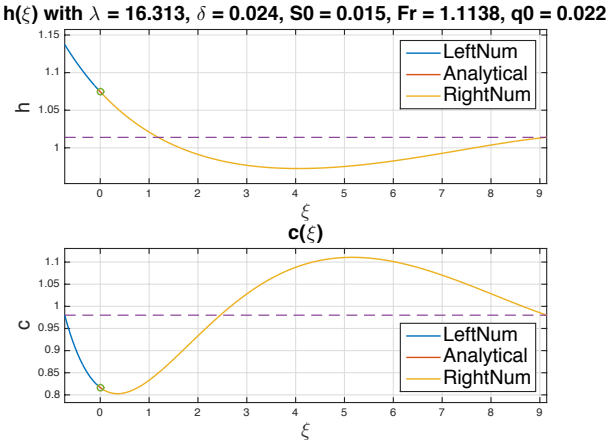

(d) Fix $S_0 = 0.0150$ and vary $q_0 = 0.11$

Figure 4.2: $h(\xi)$ vs. ξ and $c(\xi)$ vs. ξ plots for fixed Froude numbers $Fr = 1.1603$ and $Fr = 1.1138$, respectively.

In Figure 4.2, the left hand side plots are for fixed $q_0 = 0.1097\,\mathrm{m}^2\,\mathrm{s}^{-1}$ and different S_0 for two different Froude numbers (Fr), whereas the right hand side plots are for fixed $S_0 = 0.0150$ and different values of q_0, always making sure that Fr is kept fixed.

Furthermore, we produce plots that show the variation of wave speed and wavelength with the bed slope, S_0, and the water flow rate, q_0. In the top graph of Figure 4.3a we fix $q_0 = 0.1097\ \mathrm{m}^2\ \mathrm{s}^{-1}$ and vary the bed slope, S_0. Note that we had to ensure that the Froude number was $Fr > 1$ for our model to be valid since this is when antidunes form. In the bottom graph of Figure 4.3a we fix the bed slope at $S_0 = 0.0150$ and this time vary q_0. Recall that we choose the values of q_0 to ensure the Froude numbers in the top and bottom graphs of Figure 4.3a agree. The point most on the left of the upper graph of Figure 4.3a has the same Fr as the point most on the right of the lower graph, and the same holds for all pair of points.

Here we observe that the wave speed, λ, decreases when the bed slope, S_0, is increased or when the flow rate, q_0, is increased. This makes sense since if we make the bed slope steeper or increase the water flow rate, then the bed has to travel up against a higher resistance to its propagation.

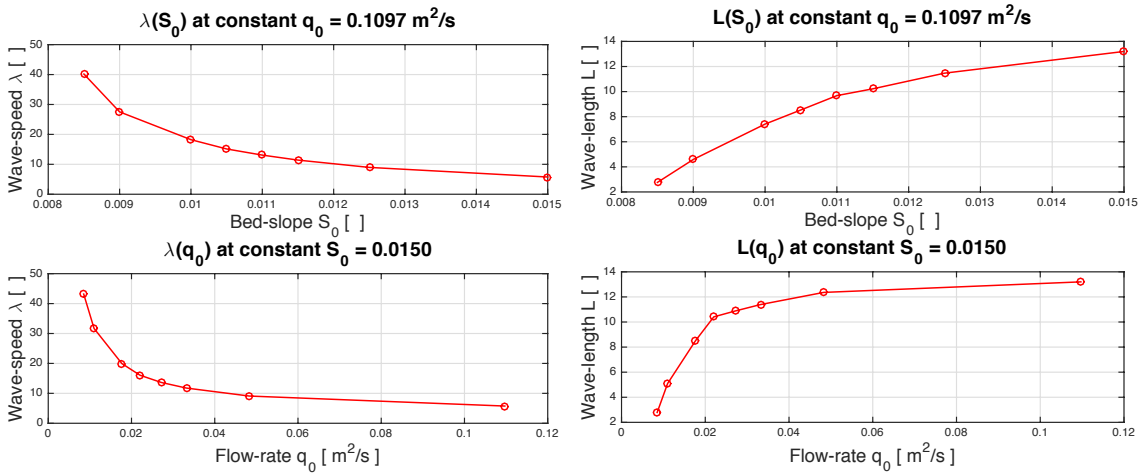

(a) Effect of changing S_0 and q_0 on λ.

(b) Effect of changing S_0 and q_0 on L.

Figure 4.3: Investigating the effect of varying the two-parameter family.

On the other hand, the wavelength, L, is proportional to the bed slope and the flow rate, since it increases with both S_0 and q_0. Again, we make sure that the Froude number matches for each pair of points and vary each parameter separately. In Figure 4.3b we see that the wavelength of the hydraulic jump increases as either the bed slope, S_0, or the water flow rate, q_0, is increased. Recall that the wavelength must satisfy condition (4.4).

5 Conclusion

In this project, we considered an extended HR model which includes the St. Venant equations and the Exner equations. After non-dimensionaling the full model and changing into a reference frame moving with the shock, we were able to produce graphs to model the behaviour of the hydraulic jumps which occur as overland flow acts on layers of soil. Numerical simulations were used to verify the results. In the process, we had to make sure that the Rankine-Hugoniot conditions derived from the leading order equations were satisfied. These were: the height of the hydraulic jump, continuity of concentration and mass conservation over the wavelength.

Although the model we considered dealt with multiple particle size classes, throughout this project we focused our numerics on a single particle size class. Therefore, future work could involve generalising these to take into account multiple particle size classes. The challenge there would be in coding the equations shown in this report for multiple classes.

In addition, the entire wavelength of the antidune was assumed to be fully covered with deposited sediment such that $H = 1$. However, it is also possible to make this more general by letting H take the form (2.3).

Finally, we explored the effect of changing parameters such as the bed slope or the flow rate on the wave speed and the wavelength of the hydraulic jump. While investigating this effect, we had to ensure that the range of Froude numbers did not fall below 1 to ensure supercritical flow – otherwise it would be uninteresting as instabilities would not grow.

Acknowledgments. I would like to thank our supervisor Professor Graham Sander for all the support he has provided throughout this project.

References

[1] A. Fowler. *Mathematical Geoscience*. Interdisciplinary Applied Mathematics. Springer London, 2011.

[2] P. B. Hairsine and C. W. Rose. Modeling water erosion due to overland flow using physical principles: 1. sheet flow. *Water resources research*, 28(1):237–243, 1992.

[3] Y. Zhong. *Modelling sediment transportation and overland flow*. PhD thesis, University of Oxford, 2013.

Appendix A Flow over Rough Surfaces–Friction Laws

In this section, we present the derivation for the two friction laws: Chézy and Manning, following [1].

A.1 Derivation of Chézy's Formula

Consider one-dimensional flow and let A denote the cross-sectional area of the flow and q denote the discharge. The mean velocity is given by

$$u = \frac{q}{A} \tag{A.1}$$

and the channel depth can be approximated by $h \sim A^{1/2}$.

We will assume that the flow is slowly varying, so we will ignore accelerations. Slow corresponds to a small Froude number

$$Fr = \frac{u}{\sqrt{gh}} = \frac{q}{h\sqrt{gh}} = \frac{q}{g^{1/2}h^{3/2}} = \frac{q}{g^{1/2}A^{3/4}}. \tag{A.2}$$

If $Fr < 1$ then we say that the flow is tranquil and if $Fr > 1$ then we say that the flow is rapid. Therefore the Froude number is a measure of the tranquility of the flow.

The force balance within a cross-section is given by

$$\tau l = \rho g A \sin\alpha = \rho g A S, \tag{A.3}$$

where $S = \sin\alpha$, and α is the downstream angle of slope, l is the wetted perimeter of a cross-section, ρ is the density, g is the gravitational acceleration and τ is the shear stress.

Shear stress can be parameterised by

$$\tau = f\rho u^2, \tag{A.4}$$

where f is the friction factor which depends on the Reynolds number and it has magnitude $f \approx 0.01$.

Let us define the hydraulic radius by

$$R = \frac{A}{l}. \tag{A.5}$$

If we substitute (A.4) in (A.3) we get after rearrangement and substituting (A.5)

$$u^2 = \frac{gAS}{lf} = \frac{gRS}{f}. \tag{A.6}$$

Therefore, we obtain that the mean velocity using Chézy is given by

$$u = \sqrt{\frac{gRS}{f}} = CR^{1/2}S^{1/2}, \tag{A.7}$$

where $C = \sqrt{\frac{g}{f}}$ is the Chézy roughness coefficient.

We can also define the discharge formula as

$$q = uA = \sqrt{\frac{gRS}{f}}A = \sqrt{\frac{gAS}{lf}}A = \sqrt{\frac{g}{lf}}A^{3/2}S^{1/2}. \tag{A.8}$$

The Froude number in terms of the hydraulic radius is

$$Fr = \frac{u}{\sqrt{gR}} = \frac{\sqrt{\frac{g}{f}}R^{1/2}S^{1/2}}{\sqrt{gR}}. \tag{A.9}$$

Thus, the Froude number becomes

$$Fr = \sqrt{\frac{S}{f}}, \tag{A.10}$$

which means that the tranquility of the flow is essentially determined by the bed slope, S and the friction factor, f.

A.2 Derivation of Manning's Formula

Alternatively, we can use a different friction correlation which was found by Manning. The difference with Chézy is that the shear stress is parameterised in this case by

$$\tau = \frac{\rho g n^2 u^2}{R^{1/3}}. \tag{A.11}$$

Using similar arguments to before, we substitute (A.11) and (A.5) in (A.3) and, we obtain

$$u^2 = \frac{R^{1/3}SA}{ln^2} = \frac{R^{4/3}S}{n^2}. \tag{A.12}$$

So the velocity for Manning's law is given by

$$u = \frac{R^{2/3}S^{1/2}}{n}. \tag{A.13}$$

If we compare (A.7) with (A.13) then we see that $C = \frac{R^{1/6}}{n}$.

Taking everything into consideration, we can provide a relationship between discharge and cross-sectional area $q = uA$ if we substitute for Chézy's (A.7) or Manning's

(A.13) velocity formula. This relationship includes the hydraulic radius, which itself can be related to the cross-sectional area through $R = \frac{A}{l}$.

We write

$$q = \frac{cA^{m+1}}{m+1}, \tag{A.14}$$

where for Chézy's law $m + 1 = \frac{3}{2}$ for canal shape cross-section or $m + 1 = \frac{5}{4}$ for circular shape cross-section and for Manning $m + 1 = \frac{5}{3}$ or $\frac{4}{3}$, respectively.

Appendix B Froude Number and Type of Flow

The magnitude of the dimensionless number called the *Froude number* which is given by $Fr = \frac{u}{\sqrt{gh}}$ determines the type of flow. The different types of flow are listed below.

1. $Fr < 1$ corresponds to subcritical flow. The ripples on water, $\sqrt{gh}$, propagate faster than the flow speed u of the stream, meaning that those ripples can move both up and down the flow. Characteristics will travel both upstream and downstream.

2. $Fr = 1$ corresponds to critical flow. This is the intermediate case.

3. $Fr > 1$ corresponds to supercritical flow. The water flows faster than ripples can propagate, and so they can only propagate downstream. The characteristics only travel downstream.

Appendix C Summary of Constants in HR Model

Summary of HR model constants

F :	fraction of excess stream power effective in detachment
J :	specific energy needed for detachment
$H \in [0, 1]$:	protection factor of cohesive layer due to deposited layer
τ :	shear stress on the soil
$\Omega = u\tau$, Ω_{cr} :	stream power on the soil and critical power, respectively
ρ, ρ_s :	water and particle density, respectively

Appendix D Deriving Equation (3.23)

Using (3.12) we can write

$$\frac{\mathrm{d}c}{\mathrm{d}\xi} = \sum_{i=1}^{I} \frac{\mathrm{d}c_i}{\mathrm{d}\xi} = \sum_{i=1}^{I} \left[\Omega \frac{H}{h} \frac{\psi_i - c_i}{\psi - c} - v_i c_i \right] = \Omega \frac{H}{h} - \sum_{i=1}^{I} v_i c_i = \frac{H}{h^{13/3}} - \sum_{i=1}^{I} v_i c_i, \quad \text{(D.1)}$$

where in the last equality we used that $\Omega = \frac{1}{h^{10/3}}$.

If we now substitute this into (3.20) then we obtain

$$\lambda\delta + \frac{\Omega_c}{h_c} - \sum_{i=1}^{I} v_i c_i^c - \frac{\lambda\delta}{h_c^{10/3}} = 0. \quad \text{(D.2)}$$

Furthermore, we can substitute these into the coupled system for c and h

$$\frac{\mathrm{d}h}{\mathrm{d}\xi} = \frac{h^3}{h^3 - Fr^2} \left(\delta + \frac{1}{\lambda} \frac{\mathrm{d}c}{\mathrm{d}\xi} - \frac{\delta}{h^{10/3}} \right) \quad \text{(D.3)}$$

to obtain the following

$$\begin{aligned} \frac{\mathrm{d}h}{\mathrm{d}\xi} &= \frac{h^3}{h^3 - Fr^2} \left(\delta + \frac{1}{\lambda} \frac{H}{h^{13/3}} - \frac{1}{\lambda} \sum_{i=1}^{I} v_i c_i - \frac{\lambda\delta}{h^{10/3}} \right) \\ &= \frac{1}{\lambda} \frac{h^3}{h^3 - Fr^2} \left(-\frac{\Omega_c}{h_c} + \sum_{i=1}^{I} v_i c_i^c + \frac{\lambda\delta}{h_c^{10/3}} + \frac{H}{h^{13/3}} - \sum_{i=1}^{I} v_i c_i - \frac{\lambda\delta}{h^{10/3}} \right) \\ &= \frac{1}{\lambda} \frac{h^3}{h^3 - h_c^3} \left(\sum_{i=1}^{I} (c_i^c - c_i) + \frac{1}{h^{13/3}} \left[H - \left(\frac{h}{h_c} \right)^{13/3} \right] - \frac{\lambda\delta}{h^{10/3}} \left[1 - \left(\frac{h}{h_c} \right)^{10/3} \right] \right). \end{aligned} \quad \text{(D.4)}$$

Note that we used $\lambda\delta = -\frac{\Omega_c}{h_c} + \sum_{i=1}^{I} v_i c_i^c + \frac{\lambda\delta}{h_c^{10/3}}$, that $\Omega_c = \frac{1}{h_c^{10/3}}$ and finally $Fr^2 = h_c^3$.

We can write this also in terms of θ, where recall that $\theta = \frac{h}{h_c}$, and so dividing (D.4) throughout by $h_c^{13/3}$ and noting that $h_c \frac{\mathrm{d}\theta}{\mathrm{d}\xi} = \frac{\mathrm{d}h}{\mathrm{d}\xi}$, yields (3.23).

Appendix E Finding the constants a_0, a_1, b_0 and b_1

We assumed that we have a series expansion of the following form

$$\frac{\sum_{i=1}^{I} v_i (c_i^c - c_i)}{\theta - 1} = a_0 + a_1(\theta - 1). \quad \text{(E.1)}$$

Therefore, (3.24) can be written as

$$h_c^{16/3} \lambda \frac{\mathrm{d}\theta}{\mathrm{d}\xi} = \frac{h_c^{13/3} \theta^3}{\theta^2 + \theta + 1} \left[a_0 + a_1(\theta - 1) \right] + \frac{1 - \theta^{13/3}}{\theta^{4/3}(\theta^3 - 1)} - \lambda\delta h_c \frac{\left(1 - \theta^{10/3}\right)}{\theta^{1/3}(\theta^3 - 1)}. \quad \text{(E.2)}$$

Note that the Taylor series expansion for $\frac{\theta^3}{\theta^2+\theta+1}$ about $\theta = 1$ is given by

$$\frac{\theta^3}{\theta^2+\theta+1} \approx \frac{1}{3} + \frac{2}{3}(\theta-1) + \mathcal{O}(\theta-1)^2. \tag{E.3}$$

Additionally, the Taylor series expansion about $\theta = 1$ for $\frac{1-\theta^{13/3}}{\theta^{4/3}(\theta^3-1)}$ is

$$\frac{1-\theta^{13/3}}{\theta^{4/3}(\theta^3-1)} \approx \frac{13}{9} - \frac{26(\theta-1)}{27} + \frac{338}{243}(\theta-1)^2 + \mathcal{O}(\theta-1)^3, \tag{E.4}$$

and the Taylor series expansion about $\theta = 1$ for $\frac{\theta^{10/3}-1}{\theta^{1/3}(\theta^3-1)}$ is

$$\frac{\theta^{10/3}-1}{\theta^{1/3}(\theta^3-1)} \approx \frac{10}{9} - \frac{5(\theta-1)}{27} + \frac{5}{243}(\theta-1)^2 + \mathcal{O}(\theta-1)^3. \tag{E.5}$$

Thus, if we combine all these we obtain

$$\begin{aligned} h_c^{16/3}\lambda\frac{\mathrm{d}\theta}{\mathrm{d}\xi} = &\left[\frac{h_c^{13/3}}{3}a_0 - \frac{13}{9} + \lambda\delta h_c\frac{10}{9}\right] \\ &+ \left[\frac{2h_c^{13/3}}{3}a_0 + \frac{h_c^{13/3}}{3}a_1 + \frac{26}{27} - \frac{5}{27}\lambda\delta h_c\right](\theta-1) + \mathcal{O}(\theta-1)^2. \end{aligned} \tag{E.6}$$

Comparing coefficients of the same order of $(\theta-1)$ we get expressions for b_0 and b_1

$$\mathcal{O}(\theta-1)^0: \qquad b_0 = \frac{h_c^{13/3}}{3}a_0 + \frac{10}{9}\lambda\delta h_c - \frac{13}{9}, \tag{E.7}$$

$$\mathcal{O}(\theta-1): \qquad b_1 = \frac{h_c^{13/3}}{3}(a_1+2a_0) - \frac{5}{27}\lambda\delta h_c + \frac{26}{27}. \tag{E.8}$$

Similarly, we need to obtain expressions for a_0 and b_0. To do that, we first consider

$$\frac{\mathrm{d}c_i(\xi_c)}{\mathrm{d}\xi} = \frac{1}{h_c^{13/3}}\frac{\psi_i - c_i^c}{\psi - c^c} - v_i c_i \tag{E.9}$$

and take the derivative of this to obtain

$$\frac{\mathrm{d}^2c_i(\xi_c)}{\mathrm{d}\xi^2} = -\frac{13}{3h_c^{13/3}}\frac{\mathrm{d}\theta(\xi_c)}{\mathrm{d}\xi}\left(\frac{\psi_i - c_i^c}{\psi - c^c}\right) - \frac{1}{h_c^{13/3}}\frac{\mathrm{d}c_i(\xi_c)}{\mathrm{d}\xi}\left(\frac{1}{\psi-c^c} - \frac{\psi_i - c_i^c}{(\psi-c^c)^2}\right) - v_i\frac{\mathrm{d}c_i(\xi_c)}{\mathrm{d}\xi}. \tag{E.10}$$

At this point we use (E.1) and the Taylor expansion of c_i around $\xi = \xi_c$

$$-\sum_{i=1}^{I} v_i(c_i^c - c_i) = (\xi-\xi_c)\sum_{i=1}^{I} v_i\frac{\mathrm{d}c_i(\xi_c)}{\mathrm{d}\xi} + \frac{(\xi-\xi_c)^2}{2}\sum_{i=1}^{I} v_i\frac{\mathrm{d}^2c_i(\xi_c)}{\mathrm{d}\xi^2}. \tag{E.11}$$

This gives

$$a_0(\theta-1)+a_1(\theta-1)^2 = \frac{\lambda h_c^{16/3}}{b_0}(\theta-1)\sum_{i=1}^{I} v_i \frac{\mathrm{d}c_i(\xi_c)}{\mathrm{d}\xi} - \frac{\lambda b_1 h_c^{16/3}}{2b_0^2}(\theta-1)^2 \sum_{i=1}^{I} v_i \frac{\mathrm{d}c_i(\xi_c)}{\mathrm{d}\xi} + \frac{1}{2}\left(\frac{\lambda h_c^{16/3}}{b_0}\right)^2 \sum_{i=1}^{I} v_i \frac{\mathrm{d}^2 c_i(\xi_c)}{\mathrm{d}\xi^2}(\theta-1)^2 + \mathcal{O}(\theta-1)^3, \quad \text{(E.12)}$$

where we used (3.28).

Again, comparing coefficients of the same order of $(\theta-1)$ we get expressions for a_0 and a_1

$$\mathcal{O}(\theta-1): \qquad a_0 = -\frac{\lambda h_c^{16/3}}{b_0}\sum_{i=1}^{I} v_i \frac{\mathrm{d}c_i(\xi_c)}{\mathrm{d}\xi} \quad \text{(E.13)}$$

$$\mathcal{O}(\theta-1)^2: \qquad a_1 = \frac{\lambda h_c^{16/3}}{2b_0^2} b_1 \sum_{i=1}^{I} v_i \frac{\mathrm{d}c_i(\xi_c)}{\mathrm{d}\xi} - \frac{1}{2}\frac{\lambda^2 h_c^{32/3}}{b_0^2}\sum_{i=1}^{I} v_i \frac{\mathrm{d}^2 c_i(\xi_c)}{\mathrm{d}\xi^2}(\theta-1)^2. \quad \text{(E.14)}$$

We choose λ and this fixed the value of c^c in

$$c^c = \lambda\delta(1-h_c^{-3}) + h_c^{-4}, \quad \text{(E.15)}$$

so we can find $\frac{\mathrm{d}c_i(\xi_c)}{\mathrm{d}\xi} = h_c^{-4} - c^c$.

Furthermore, we can solve simultaneously

$$b_0 = \frac{h_c^4}{3}a_0 + \lambda\delta h_c - \frac{4}{3} \quad \text{and} \quad a_0 = -\frac{\lambda h_c^5}{b_0}\frac{\mathrm{d}c_i(\xi_c)}{\mathrm{d}\xi}, \quad \text{(E.16)}$$

to get first a quadratic for b_0 given by

$$b_0^2 + \left(\frac{4}{3} - \lambda\delta h_c\right) b_0 + \frac{\lambda h_c^9}{3}\frac{\mathrm{d}c_i(\xi_c)}{\mathrm{d}\xi} = 0. \quad \text{(E.17)}$$

Solving the quadratic yields

$$b_0 = \frac{1}{2}\left[\left(\lambda\delta h_c - \frac{4}{3}\right) \pm \sqrt{\left(\lambda\delta h_c - \frac{4}{3}\right)^2 - 4\left(\frac{\lambda h_c^9}{3}\frac{\mathrm{d}c_i(\xi_c)}{\mathrm{d}\xi}\right)}\right]. \quad \text{(E.18)}$$

Having determined b_0 we can now find a_0.

In a similar manner, we can substitute

$$b_1 = \frac{h_c^4}{3}(a_1 + 2a_0) + \frac{2}{3} \quad \text{(E.19)}$$

into the equation for a_1 that is given by

$$a_1 = -\frac{b_1 \lambda h_c^5}{2b_0^2}\frac{\mathrm{d}c_i(\xi_c)}{\mathrm{d}\xi} - \frac{\lambda^2 h_c^{10}}{2b_0^2}\frac{\mathrm{d}^2 c_i(\xi_c)}{\mathrm{d}\xi^2}. \tag{E.20}$$

Solving for a_1 yields

$$a_1 = \frac{1}{1+\frac{\lambda h_c^9}{6b_0^2}\frac{\mathrm{d}c_i(\xi_c)}{\mathrm{d}\xi}}\left[-\frac{\lambda h_c^5}{2b_0^2}\frac{\mathrm{d}c_i(\xi_c)}{\mathrm{d}\xi}\left\{\frac{2a_0 h_c^4}{3}+\frac{2}{3}\right\} - -\frac{\lambda^2 h_c^{10}}{2b_0^2}\frac{\mathrm{d}^2 c_i(\xi_c)}{\mathrm{d}\xi^2}\right]. \tag{E.21}$$

All the constants in the expression for b_1 are now determined.

Appendix F Deriving Equation (3.27)

We start with the differential equation

$$h_c^{16/3}\lambda\frac{\mathrm{d}(\theta-1)}{\mathrm{d}\xi} = b_0 + b_1(\theta-1) \tag{F.1}$$

and we rearrange it to get

$$\frac{\mathrm{d}(\theta-1)}{\mathrm{d}\xi} - \frac{b_1(\theta-1)}{h_c^{16/3}\lambda} = \frac{b_0}{h_c^{16/3}\lambda}. \tag{F.2}$$

This is a first order differential equation that can be solved using an integrating factor (I. F.). We take the integrating factor to be

$$\text{I.F.} = \exp\left(-\frac{b_1}{h_c^{16/3}\lambda}\xi\right). \tag{F.3}$$

If we multiply now the differential equation (F.2) by the integrating factor (F.3) then we obtain

$$\frac{\mathrm{d}}{\mathrm{d}\xi}\left[\exp\left(-\frac{b_1}{h_c^{16/3}\lambda}\xi\right)(\theta-1)\right] = \frac{b_0}{h_c^{16/3}\lambda}\exp\left(-\frac{b_1}{h_c^{16/3}\lambda}\xi\right), \tag{F.4}$$

and integrating (F.4), the equation becomes

$$\exp\left(-\frac{b_1}{h_c^{16/3}\lambda}\xi\right)(\theta-1) = -\frac{b_0}{b_1}\exp\left(-\frac{b_1}{h_c^{16/3}\lambda}\xi\right) + C, \tag{F.5}$$

where C is the constant of integration. At this point, we multiply (F.5) by $\exp\left(-\frac{b_1}{h_c^{16/3}\lambda}\xi\right)$ to obtain

$$\theta - 1 = -\frac{b_0}{b_1} + C\exp\left(\frac{b_1}{h_c^{16/3}\lambda}\xi\right). \tag{F.6}$$

To determine the constant of integration we need to use the fact that at $\theta = 1$ we have that $\xi = \xi_c$. This yields

$$C = \frac{b_0}{b_1} \exp\left(-\frac{b_1}{h_c^{16/3}\lambda}\xi_c\right). \tag{F.7}$$

Substituting the constant found into (F.6), gives

$$\begin{aligned}
\theta - 1 &= -\frac{b_0}{b_1} + \exp\left(\frac{b_1}{h_c^{16/3}\lambda}\xi\right) \exp\left(-\frac{b_1}{h_c^{16/3}\lambda}\xi_c\right) \frac{b_0}{b_1} \\
&= -\frac{b_0}{b_1} + \frac{b_0}{b_1} \exp\left(\frac{b_1}{h_c^{16/3}\lambda}(\xi - \xi_c)\right) \\
&= -\frac{b_0}{b_1} + \frac{b_0}{b_1}\left[1 + \frac{b_1}{h_c^{16/3}\lambda}(\xi - \xi_c) + \frac{b_1^2}{2h_c^{32/3}\lambda^2}(\xi - \xi_c)^2 + \dots\right] \\
&= \frac{b_0}{h_c^{16/3}\lambda}(\xi - \xi_c) + \frac{b_0 b_1}{2h_c^{32/3}\lambda^2}(\xi - \xi_c)^2 + \dots,
\end{aligned} \tag{F.8}$$

where in the third equality we used the series expansion of the exponential function.